



## Original Article

# Xenogeneic transplantation of human adipose-derived stem cell sheets accelerate angiogenesis and the healing of skin wounds in a Zucker Diabetic Fatty rat model of obese diabetes



Mariko Hamada <sup>a, b</sup>, Takanori Iwata <sup>b, \*\*</sup>, Yuka Kato <sup>a, b</sup>, Kaoru Washio <sup>b</sup>,  
Shunichi Morikawa <sup>c</sup>, Hiroyuki Sakurai <sup>d</sup>, Masayuki Yamato <sup>b</sup>, Teruo Okano <sup>b, \*</sup>,  
Yasuko Uchigata <sup>a</sup>

<sup>a</sup> Diabetic Center, Tokyo Women's Medical University, School of Medicine, Tokyo, Japan

<sup>b</sup> Institute of Advanced Biomedical Engineering and Science, Tokyo Women's Medical University (TWMU), Tokyo, Japan

<sup>c</sup> Department of Anatomy and Developmental Biology, Tokyo Women's Medical University, School of Medicine, Tokyo, Japan

<sup>d</sup> Department of Plastic Surgery, Tokyo Women's Medical University, School of Medicine, Tokyo, Japan

## ARTICLE INFO

*Article history:*

Received 28 December 2016

Received in revised form

15 February 2017

Accepted 17 February 2017

*Keywords:*

Diabetic foot ulcers

Adipose-derived stem cell

Cell sheet

Wound healing

Xenogeneic transplantation

## ABSTRACT

**Introduction:** Diabetic patients with foot ulcers often suffer impaired wound healing due to diabetic neuropathy and blood flow disturbances. Direct injection of human adipose-derived stem cells (hASCs) effectively accelerates wound healing, although hASCs are relatively unstable.

**Methods:** We developed an optimized protocol to engineer hASC sheets using temperature-responsive culture dishes to enhance the function and stability of transplanted cells used for regenerative medicine. Here, we evaluated the efficacy of hASC sheets for enhancing wound healing. For this purpose, we used a xenogeneic model of obese type 2 diabetes, the Zucker Diabetic Fatty rat (ZDF rat), which displays full-thickness skin defects. We isolated hASCs from five donors, created hASC sheets, and transplanted the hASC sheets along with artificial skin into full-thickness, large skin defects (15-mm diameter) of ZDF rats.

**Results:** The hASC sheets secreted angiogenic growth factors. Transplantation of the hASC sheets combined with artificial skin increased blood vessel density and dermal thickness, thus accelerating wound healing compared with that in the controls. Immunohistochemical analysis revealed significantly more frequent neovascularization in xenografted rats of the transplantation group, and the transplanted hASCs were localized to the periphery of new blood vessels.

**Conclusion:** This xenograft model may contribute to the use of human cell tissue-based products (hCTPs) and the identification of factors produced by hCTPs that accelerate wound healing.

© 2017, The Japanese Society for Regenerative Medicine. Production and hosting by Elsevier B.V. This is an open access article under the CC BY-NC-ND license (<http://creativecommons.org/licenses/by-nc-nd/4.0/>).

**Abbreviations:** hASCs, Human adipose-derived stem cells; ZDF rats, Zucker Diabetic Fatty Rats; AA, L-ascorbic acid phosphate magnesium salt; CFA, Colony-forming assay; ITS, Insulin-Transferrin-Selenium.

\* Corresponding author. Institute of Advanced Biomedical Engineering and Science, Tokyo Women's Medical University (TWMU), 8-1 Kawada-cho, Shinjuku-ku, Tokyo 162-8666, Japan. Fax: +81 3 3359-6046.

\*\* Corresponding author. Institute of Advanced Biomedical Engineering and Science, Tokyo Women's Medical University (TWMU), 8-1 Kawada-cho, Shinjuku-ku, Tokyo 162-8666, Japan. Fax: +81 3 3359-6046.

**E-mail addresses:** [mhamada.dmc@twmu.ac.jp](mailto:mhamada.dmc@twmu.ac.jp) (M. Hamada), [iwata.takanori@twmu.ac.jp](mailto:iwata.takanori@twmu.ac.jp) (T. Iwata), [kato.yuka@twmu.ac.jp](mailto:kato.yuka@twmu.ac.jp) (Y. Kato), [washio.kaoru@twmu.ac.jp](mailto:washio.kaoru@twmu.ac.jp) (K. Washio), [shun@research.twmu.ac.jp](mailto:shun@research.twmu.ac.jp) (S. Morikawa), [sakurai.hiroyuki@twmu.ac.jp](mailto:sakurai.hiroyuki@twmu.ac.jp) (H. Sakurai), [yamato.masayuki@twmu.ac.jp](mailto:yamato.masayuki@twmu.ac.jp) (M. Yamato), [tokano@twmu.ac.jp](mailto:tokano@twmu.ac.jp) (T. Okano), [uchigata.dmc@twmu.ac.jp](mailto:uchigata.dmc@twmu.ac.jp) (Y. Uchigata).

Peer review under responsibility of the Japanese Society for Regenerative Medicine.

<http://dx.doi.org/10.1016/j.reth.2017.02.002>

2352-3204/© 2017, The Japanese Society for Regenerative Medicine. Production and hosting by Elsevier B.V. This is an open access article under the CC BY-NC-ND license (<http://creativecommons.org/licenses/by-nc-nd/4.0/>).

## 1. Introduction

The International Diabetes Federation reported that there were 400 million patients with diabetes worldwide in 2015 [1] and approximately 15%–25% of these patients suffer from foot ulcers [2]. Therefore, the number of patients with diabetes, including those affected by foot ulcers, will increase. Moreover, 7%–20% of patients with diabetic foot ulcers undergo amputation of their lower extremities [3]. Thus, there is an urgent need to establish effective therapies to treat diabetic foot ulcers.

Wound healing involves complex biological and molecular responses to tissue injury [4]. Under diabetic conditions, evidence indicates that multiple factors such as prolonged inflammation, decreased collagen synthesis, decreased growth factor secretion, and impaired neovascularization delay wound healing [5]. Treatment with artificial skin accelerates the synthesis of new connective tissue matrices and regenerates the dermis [6]. However, using only artificial skin to treat relatively large wounds caused by diabetic foot ulcers is difficult because of diabetic neuropathy and impaired blood flow.

Cell-based therapy using human adipose-derived stem cells (hASCs) represents a new approach to enhance wound healing [7,8]. However, cells in a single-cell suspension of hASCs migrate from the injection site to the wound area through diffusion [9,10]. To decrease the rate of migration of hASCs into the wound, we developed cell-sheet engineering using temperature-responsive culture dishes coated with the temperature-responsive polymer *N*-isopropylacrylamide. The grafted polymer layer allows cultured cells to adhere at 37 °C and spontaneously detach from the surface at <32 °C. The dish enables nonenzymatic, noninvasive harvesting of the cells as a sheet [11].

Clinical studies using cell sheets made of stem cells indicate the efficacy of this technique for treating esophageal ulcerations [12], periodontitis [13], corneal dysfunction [14], and myocardial infarction [15]. We previously generated rat adipose-derived stem cell (rASC) sheets and found that transplantation of the rASC sheet increased blood vessel density and dermal thickness, which were associated with accelerated wound healing compared with controls [16]. These results suggest that the rASC sheet combined with artificial skin offers a new approach to treat diabetic foot ulcers. We tried to create hASCs sheets under clinical settings. Moreover, the protocol of creating hASC sheets has not been reported yet.

The aim of this study was to establish the optimum protocol for creating hASC sheets and to evaluate their efficacy for accelerating wound healing. For this purpose, we employed the Zucker Diabetic Fatty Rat (ZDF rat) with full-thickness skin defects to serve as a xenogeneic model of type 2 diabetes.

## 2. Materials and methods

### 2.1. Animals

Male ZDF rats (ZDF-*Lepr*<sup>fa</sup>/CrIj) aged 16 weeks (Charles River Laboratories Japan, Kanagawa, Japan) were used to establish a wound-healing model of type 2 diabetes and obesity. The Animal Welfare Committee of Tokyo Women's Medical University approved the use of rats. We used only male rats in this study, considering that estrogen modifies wound healing [17].

### 2.2. Human subjects

This study was conducted according to the principles of the Declaration of Helsinki. The Institutional Review Board of the Tokyo Women's Medical University approved the collection of human samples and all donors provided written informed consent. Adipose tissues were present in samples of lower abdominal subcutaneous fat collected from five donors with cancer who underwent breast augmentation after mastectomy. Clinical data for each patient are presented in Table 1.

### 2.3. Isolation and culture of hASCs

Adipose tissue was digested using collagenase NB6 GMP (0.3 U/g tissue; Serva Electrophoresis, Heidelberg, Germany), at 37 °C for 1 h [18], followed by centrifugation at 700 × *g* for 5 min at 22 °C. The cells were added to a T75 flask (Falcon) and allowed to adhere to the surface. The flask contained  $\alpha$ -MEM with GlutaMAX (Life Technologies, Carlsbad, CA, USA), 10% FBS (Moregate Biotech, Queensland, Australia), 0.1% gentamicin (MSD, Tokyo, Japan), and 0.05% amphotericin B (Bristol-Myers Squibb, Tokyo, Japan) at 37 °C in an atmosphere containing 5% CO<sub>2</sub> for 24 h (Passage 0). After three washes with phosphate-buffered saline (PBS) (Life Technologies, Grand Island, NY, USA), new fresh medium was added. The cells were subcultured using 0.25% trypsin-ethylenediaminetetraacetic acid (EDTA; Life Technologies) every 3 days until Passage 2 and the cryopreserved using a CELL BANKER 1 (Nippon Zenyaku Kogyo, Fukushima, Japan). The cells were stored at –80 °C for at least 1 month (Fig. 1a).

### 2.4. Proliferation assay

The numbers of cells from five donors per hASC sheet were counted using a hemocytometer at days 0, 3, 5, 7, 10, 14, and 17 after seeding on each of three temperature-responsive culture dishes (UPCell; CellSeed, Tokyo, Japan).

**Table 1**  
Clinical characteristics of donors.

Number	Donor 1	Donor 2	Donor 3	Donor 4	Donor 5
Age (years)	66	52	57	42	46
Sex	F	F	F	F	F
BMI (kg/m <sup>2</sup> )	21.1	26.5	24.3	23.8	19.3
Amount of adipose tissue (mg)	2102	3556	3604	3416	3549
Fasting blood glucose (mmol/L)		5.4	5.2	4.8	5.4
Postprandial blood glucose (mmol/L)	6.3				
HbA <sub>1c</sub> (%)	5.7	5.8	5.5	5.5	5.5
HbA <sub>1c</sub> (mmol/mol)	39	40	37	37	37
Creatinine ( $\mu$ mol/L)	63	59	44	55	63
LDL cholesterol (mmol/L)	3.7	5.4	3.7	2.3	2.8
HDL cholesterol (mmol/L)	1.9	1.5	1.6	1.7	2
Triglycerides (mmol/L)	1.17	1.55	1.75	0.79	0.51

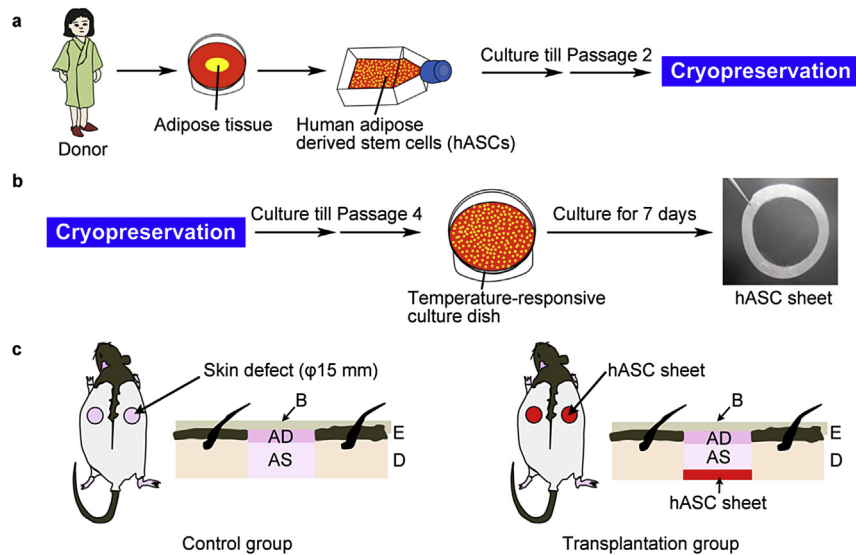


**Fig. 1.** Transplantation procedure was performed using an hASC sheet combined with an artificial skin that was used to cover a full-thickness skin wound of a ZDF rat. (a) hASCs were isolated and seeded, and then cultured until Passage 2, and cryopreserved. (b) hASCs were thawed, cultured until Passage 4, and seeded at  $1.0 \times 10^5$  cells per temperature-responsive culture dish at  $37^\circ\text{C}$  for 7 days. (c) The hASC sheet was directly transplanted onto a 15-mm diameter full-thickness skin wound created on the backs of ZDF rats that were covered by an artificial skin in the transplantation group ( $n = 4$ ). Only artificial skin was transplanted onto the wounds in the control group ( $n = 4$ ). B: bandage, AD: adhesive dressing, E: epidermis, D: dermis.

### 2.5. Colony-forming assay

After cryopreservation, the cells isolated from the 5 donors were thawed and cultured in complete medium ( $\alpha$ -MEM with GlutaMAX, 20% FBS, 0.1% gentamicin, and 0.05% amphotericin B) at  $37^\circ\text{C}$  in an atmosphere containing 5%  $\text{CO}_2$ . Passage-4 cells were used for the experiments. The cells (100 cells in a 60-cm<sup>2</sup> dish) were seeded in each of three dishes per donor and cultured in complete medium for 7 days. The cells were stained with 0.5% crystal violet (Kanto Chemical, Tokyo, Japan) in methanol for 5 min, washed twice with distilled water, and the number of colonies was counted.

### 2.6. Differentiation assays

Differentiation assays using the cells isolated from the 5 donors were performed three times per donor as previously described [19]. For adipogenesis, the cells (100 cells added to a 60-cm<sup>2</sup> dish) were cultured in complete medium. On day 7, the medium was replaced with adipogenic medium as follows: complete medium containing 0.5 mmol/L isobutyl-methyl xanthine (Sigma–Aldrich, St. Louis, MO, USA), 100 nmol/L dexamethasone (DEX) (Fuji Pharma, Tokyo, Japan), and 50  $\mu\text{mol/L}$  indomethacin (Wako Pure Chemical, Osaka, Japan). After 21 days, the cells were fixed with 4% paraformaldehyde (PFA) for 1 h and stained with Oil Red-O solution (Wako Pure Chemical). To induce osteogenesis, the cells (50 cells added to a 60-cm<sup>2</sup> dish) were cultured in complete medium for 7 days and the medium was then replaced with osteogenic medium as follows: complete medium containing 10 mmol/L  $\beta$ -glycerophosphate (Sigma–Aldrich), 10 nmol/L DEX, and 82  $\mu\text{g/mL}$  L-ascorbic acid phosphate magnesium salt n-Hydrate (AA) (Wako). After 21 days, the cells were stained with 1% alizarin red S solution, and the number of stained colonies was counted. The Oil Red-O-positive rate or the alizarin red S-positive rate was calculated by dividing the number of each positive colonies by the number of CFA ( $n = 3$ ).

To induce chondrogenesis, 250,000 cells were placed in a 15-mL polypropylene tube (Becton Dickinson, Mountain View, CA, USA)

and centrifuged at  $450 \times g$  for 10 min. The pellet was cultured for 21 days in chondrogenic medium as follows: high-glucose Dulbecco's modified Eagle's medium (Invitrogen) containing 500 ng/mL bone morphogenetic protein 2 (R&D Systems, Minneapolis, MN, USA), 10 ng/mL transforming growth factor  $\beta 3$  (R&D Systems), 100 nmol/L DEX, 82  $\mu\text{g/mL}$  AA, 40  $\mu\text{g/mL}$  proline, 100  $\mu\text{g/mL}$  pyruvate, and 50 mg/mL Insulin-Transferrin-Selenium (ITS) + Premix (Becton Dickinson). For immunohistochemical analysis, the pellets were embedded in OCT compound (Sakura Finetek; Torrance, CA, USA), cut into 5- $\mu\text{m}$ -thick sections using a cryostat (Leica CM 1850; FINETEC, Tokyo, Japan), and stained with 1% toluidine blue or 0.1% safranin O.

### 2.7. Karyotype analysis

Fifty cells from each hASC culture (Donors 1–5) were analyzed using G-banding (Nihon Gene Research Laboratories, Miyagi, Japan) to determine their karyotypes.

### 2.8. Flow cytometry

Seven days after seeding, the hASC sheets from five donors were digested with collagenase NB6 GMP and 0.25% trypsin-EDTA as previously described [20]. The cells ( $1 \times 10^6$ ) were suspended in 100  $\mu\text{L}$  of PBS containing 10  $\mu\text{g/mL}$  of each specific antibody (Table 2) and incubated for 30 min at  $4^\circ\text{C}$ . The cells were then

**Table 2**  
Fluorescein isothiocyanate (FITC) – conjugated antibodies used for flow cytometry.

Target	Catalog no.	Isotype control	Source
CD11b	555388	Mouse IgG	BD Pharmingen <sup>a</sup>
CD29	555443	Mouse IgG	BD Pharmingen <sup>a</sup>
CD31	555445	Mouse IgG	BD Pharmingen <sup>a</sup>
CD44	550989	Mouse IgG	BD Pharmingen <sup>a</sup>
CD45	555482	Mouse IgG	BD Pharmingen <sup>a</sup>
CD90	555595	Mouse IgG	BD Pharmingen <sup>a</sup>

<sup>a</sup> BD Pharmingen, Franklin Lakes, NJ, USA.

washed and suspended in 1 mL of PBS with 10% FBS. Cell fluorescence was determined using a Gallios flow cytometer (Beckman Coulter, CA, USA) and analyzed using Gallios and Kaluza software (Beckman Coulter).

### 2.9. Cytokine secretion by hASC sheets

Conditioned medium (Donors 1–5) was collected from each culture on days 3, 5, 7, and 10 after seeding on temperature-responsive culture dishes. Each sample was centrifuged at  $300 \times g$  for 3 min at  $4^\circ\text{C}$ , and the supernatant was stored at  $-80^\circ\text{C}$ . The levels of vascular endothelial growth factor (VEGF), insulin-like growth factor-1 (IGF-1), keratinocyte growth factor (KGF), hepatocyte growth factor (HGF), fibroblast growth factor-2 (FGF-2), platelet-derived growth factor-BB (PDGF-BB), and epidermal growth factor (EGF) were determined using ELISA kits (R&D Systems).

### 2.10. Generation of hASC sheets

One hASC (Donor 4) was chosen for the transplantation study according to the results of *in vitro* experiments (Figs. 2 and 3). The hASCs ( $1.0 \times 10^5$ ) were seeded in 35-mm diameter temperature-

responsive culture dishes followed by culture in complete medium. After 3 days, the medium was replaced with complete medium containing  $82 \mu\text{g/mL}$  AA and incubated for 4 days. The hASCs were then cultured on temperature-responsive dishes incubated at  $20^\circ\text{C}$  in  $5\% \text{CO}_2$  atmosphere. The cells formed a contiguous cell sheet and spontaneously detached (Fig. 1b).

### 2.11. Transplantation of hASC sheets onto full-thickness skin defects in ZDF rats

Male ZDF rats ( $n = 4$ ) aged 16 weeks (weight range, 520–710 g) were used for transplantation experiments. ZDF rats were anesthetized by inhalation of 4% isoflurane (Pfizer) and the skin was shaved. The blood glucose levels of the ZDF rats were measured using a blood glucose monitor (Glutest Neo Sensor; Sanwa Kagaku Kenkyusho, Nagoya, Japan) and their body weights were measured before surgery and after they were sacrificed. Next, two circular full-thickness skin defects on the back were created using a 15-mm diameter skin punch, 3-cm caudal to the intrascapular region, and defects were separated by  $\geq 1$  cm [21] (Fig. 1c). In the engrafted rats (transplantation group,  $n = 4$  per group), one hASC sheet ( $7 \times 10^5$  cells) was directly transplanted onto the defect and artificial skin (Pelnac; Smith & Nephew, Tokyo, Japan) 15-mm diameter

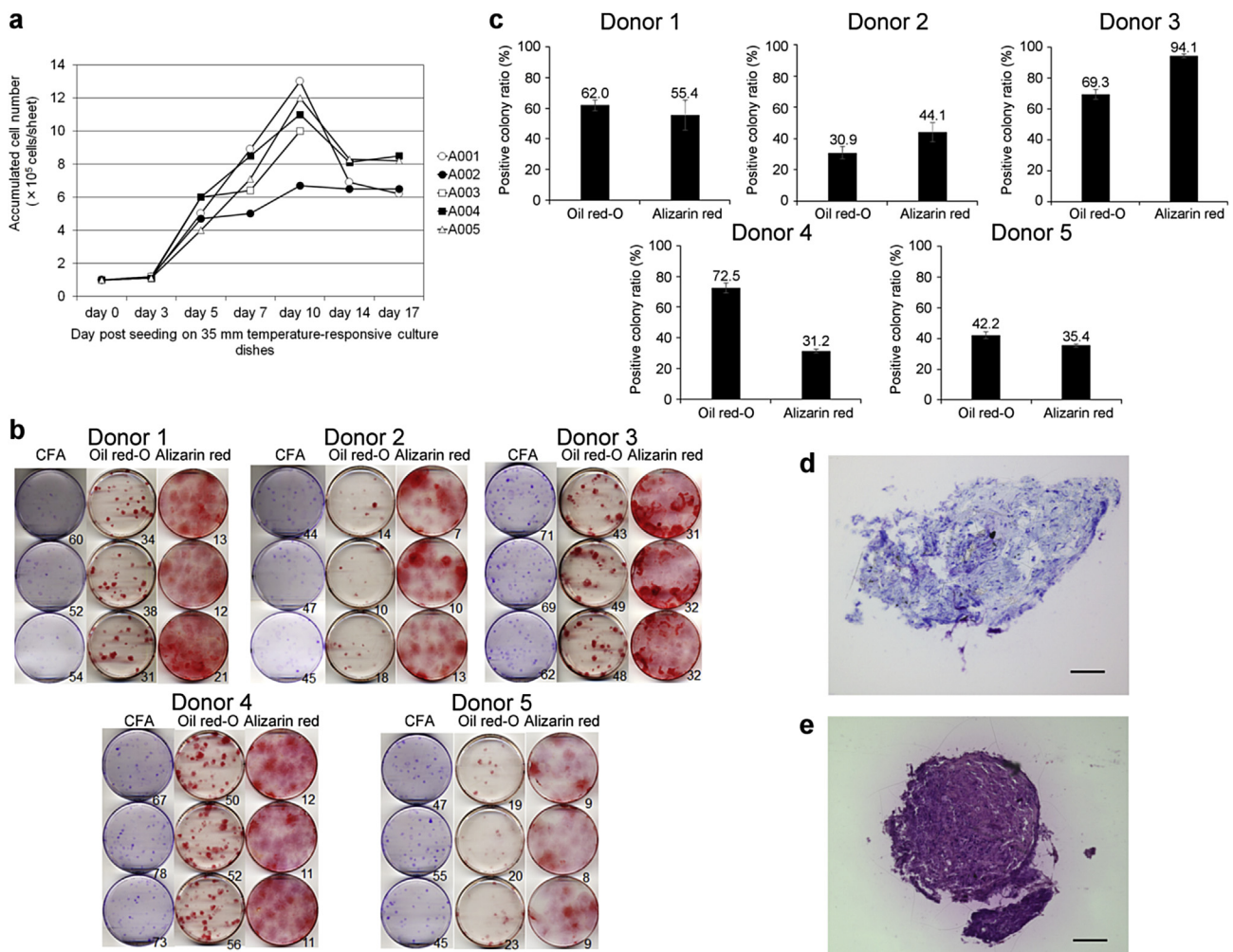


**Fig. 2.** Proliferation, self-renewal ability, and multilineage differentiation of hASCs. (a) Number of hASCs per hASC sheet. (b) CFA and adipogenic and osteogenic differentiation assays of hASCs of five donors. Crystal violet staining was performed for the CFA on day 7 and Oil Red-O and alizarin red S staining were performed on day 28 ( $n = 3$ ). (c) The ratio of Oil Red-O-positive colonies and alizarin red S-positive colonies was calculated ( $n = 3$ ). (d) To evaluate chondrogenic differentiation, hASCs in a pellet were stained with toluidine blue or safranin O, respectively. Scale bar =  $100 \mu\text{m}$ .

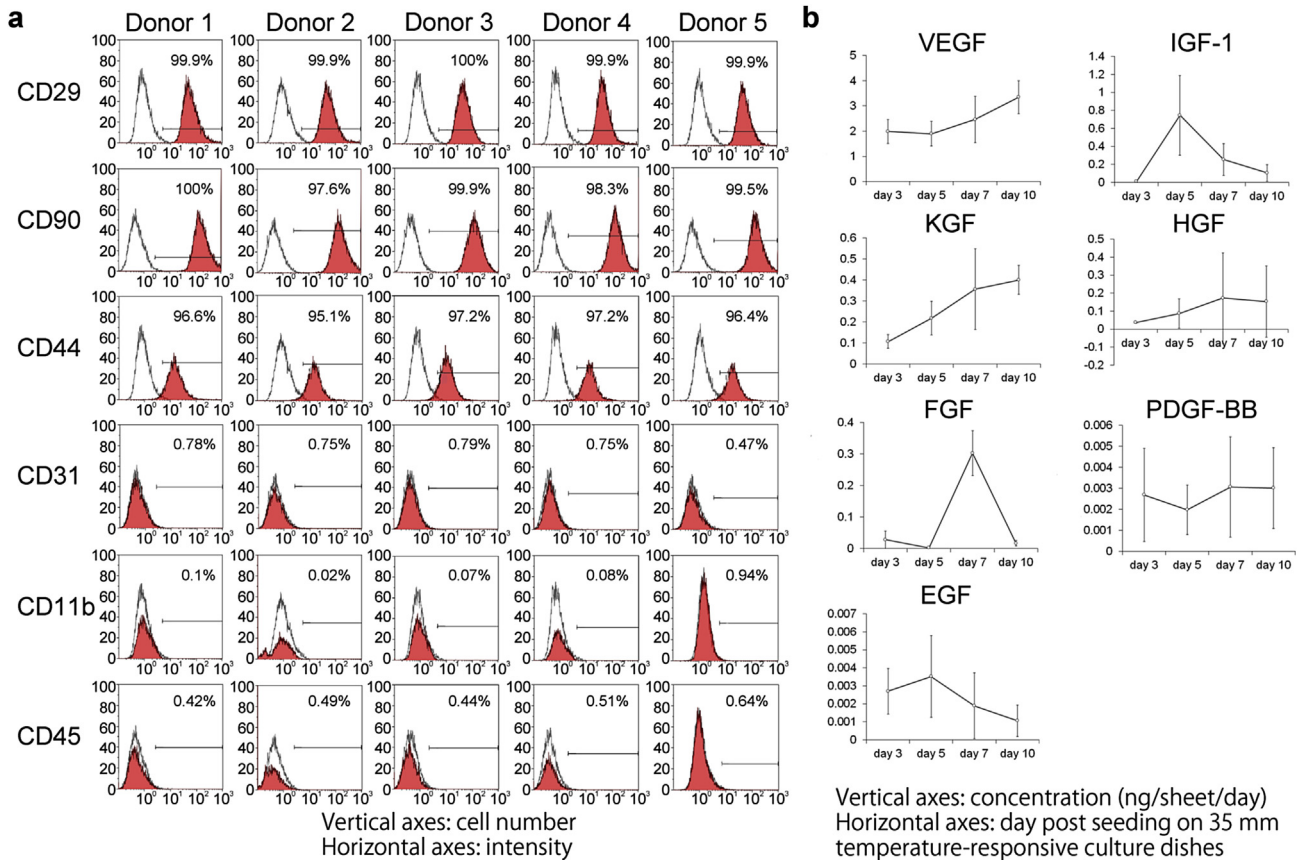


**Fig. 3.** Flow cytometric analysis of surface antigens expressed by hASCs. (a) hASCs expressed CD29, CD44, and CD90 but did not express detectable levels of CD11b, CD31, and CD45. (b) The levels of human VEGF, HGF, FGF-2, IGF-1, EGF, PDGF-BB, and KGF were determined using quantitative ELISA kits. The values shown represent the mean  $\pm$  SD.

was placed onto the hASC sheet. In the control group ( $n = 4$  per group), only the artificial skin covered on the defects. Next, a  $15 \times 15$  mm nonadhesive dressing (Hydrosite plus; Smith & Nephew) was placed on the artificial skin applied to the test and control rats and then covered with bandages (Hilate; Iwatsuki, Tokyo, Japan) to protect the wound and avoid dislocation (Fig. 1c).

### 2.12. Measurement of wounds and wound-closure time

The wounds were observed every 3 days until they completely closed. The wound-closure time was defined as when the wound was completely epithelialized. The wound area was quantified using ImageJ software (National Institutes of Health, Bethesda, MD, USA) in each ZDF rat at each observation.

### 2.13. Immunohistochemistry

Four ZDF rats in each group were sacrificed 14 days after transplantation. Following fixation with 4% PFA for 30 min at  $4^\circ\text{C}$ , the wound tissues were washed with PBS and immersed in PBS containing 30% sucrose at  $4^\circ\text{C}$  for 24 h. The wound tissues were embedded in Tissue-Tek OCT compound (Sakura Finetek), snap-frozen in liquid nitrogen, and cut into  $14\text{-}\mu\text{m}$  thick sections using a cryostat. The frozen sections were stained with hematoxylin and eosin stain (H–E stain) for histological analysis and processed for immunohistochemistry. The frozen sections were incubated in 4% Block Ace (Dainippon Seiyaku, Osaka, Japan) to block nonspecific immunoreactions and stained with primary antibodies in PBS containing 1% bovine serum albumin (Sigma–Aldrich) at  $4^\circ\text{C}$  overnight. Used primary antibodies were as follows: Rabbit anti-human CD31

(1:50; RB-10333-P, Thermo Fisher Scientific Anatomical Pathology, Fremont, CA, USA) and mouse anti-human STEM121 (1:50; Y40410, Takara Bio, Shiga, Japan). They were used to quantify vascularization in the wound and detect the transplanted hASCs, respectively. After three washes with PBS, specimens were incubated with a biotinylated anti-rabbit antibody (1:200; 711-066-152, Jackson ImmunoResearch, West Grove, PA, USA) and a Cy3-conjugated anti-mouse secondary antibody (1:200; 715-166-151, Jackson ImmunoResearch) for 3 h at room temperature. The biotinylated antibody was then visualized by incubation with Alexa Fluor 488-conjugated streptavidin (1:1000; 016-540-084, Jackson ImmunoResearch) for 1 h at room temperature. H–E stained sections and sections reacted with antibodies were examined using a Keyence BZ-9000 fluorescence microscope (Keyence Corp, Chicago, USA).

### 2.14. Tissue measurements

Dermal thickness and the blood vessel density were measured 14 days after transplantation. The dermal thicknesses of three randomly selected points of H–E stained sections were measured. The relative area of CD31-positive blood vessels (VA) was calculated as follows:  $VA(\%) = VA_{act}/A_f \times 100$ , ( $VA_{act}$ , CD31-positive vessels;  $A_f$ , area of the field). The average of the six areas in the two wounds (three areas per wound) of each ZDF rat was recorded as the blood vessel density.

### 2.15. Statistical analysis

The data are expressed as the mean  $\pm$  standard deviation (SD). All samples were analyzed using the Student's *t*-test and  $p < 0.05$  was considered significant.

### 3. Results

#### 3.1. Characterization of hASCs

The averages of the hASCs per sheet ( $n = 5$ ) were  $1.0 \times 10^5$ ,  $1.14 \times 10^5$ ,  $5.14 \times 10^5$ ,  $7.18 \times 10^5$ ,  $10.5 \times 10^5$ ,  $7.45 \times 10^5$ , and  $7.35 \times 10^5$  cells on days 0, 3, 5, 7, 10, 14, and 17, respectively. The number of hASCs per sheet gradually increased until day 10 (Fig. 2a). The hASC sheet from Donor 3 shrank on day 10. The hASCs formed colonies and differentiated along the pathways of adipogenesis, osteogenesis, and chondrogenesis (Fig. 2b–e). Flow cytometric analysis detected that CD29-, CD90-, and CD44-positive cells occupied more than 90% of all hASCs, while CD11b-, CD31-, and CD45-positive cells occupied less than 1% (Fig. 3a). These results are consistent with the characteristics of hASCs that meet the standard minimal criteria of the phenotype of mesenchymal stem cells (MSCs) defined by Dominici et al. [22].

#### 3.2. hASCs secrete multiple growth factors

ELISA assays revealed that the hASCs secreted VEGF, IGF-1, KGF, HGF, FGF, PDGF-BB, and EGF. The average of maximum time of secretion of these cytokines was  $7.29 \pm 2.06$  days after seeding (Fig. 3b). Accordingly, cell sheets were harvested on day 7 for the transplantation study.

#### 3.3. Karyotype analysis

G-banding of hASCs (Donors 1–5) revealed that the number, banding, and shape of the chromosomes of each hASC sample were normal (Fig. 4).

#### 3.4. Wound healing in vivo

The average wound areas on days 0, 3, 7, 10, 14, 17, 21, and 24 ( $n = 4$ ) after transplantation were  $2.32 \pm 0.20$ ,  $1.90 \pm 0.33$ ,  $1.66 \pm 0.39$ ,  $1.21 \pm 0.50$ ,  $0.55 \pm 0.38$ ,  $0.21 \pm 0.14$ ,  $0.11 \pm 0.10$ , and  $0.07 \pm 0.04$  cm<sup>2</sup> in the transplantation group, respectively, and  $2.32 \pm 0.23$ ,  $2.15 \pm 0.26$ ,  $2.00 \pm 0.25$ ,  $1.60 \pm 0.34$ ,  $1.12 \pm 0.35$ ,  $0.88 \pm 0.25$ ,  $0.49 \pm 0.17$ , and  $0.30 \pm 0.06$  cm<sup>2</sup> in the control group,

respectively. Wound healing was significantly accelerated in the transplantation group compared with the control group from day 3 onward (Fig. 5a and b). The average complete wound closure time was significantly shorter in the transplantation group ( $24.75 \pm 5.33$  days) compared with that of the control group ( $47.25 \pm 8.33$  days) (Fig. 5c). Clinical signs of immunorejection such as erythema, inflammation, and necrosis were not observed in either group during the experiment. The average blood glucose levels ( $402.78 \pm 120.19$  mg/dL and  $437.22 \pm 90.06$  mg/dL in the transplantation and control groups, respectively) were not significantly different. The blood glucose levels of the groups were  $\geq 300$  mg/dL.

#### 3.5. Histological and immunohistochemical analyses

H–E-stained specimens 14 days after transplantation (Fig. 6a) revealed that the dermal thickness of the transplantation group ( $1.69 \pm 0.72$  mm) was significantly higher compared with that of the control group ( $1.10 \pm 0.32$  mm) (Fig. 6c). Immunohistochemical analysis revealed the presence of CD31-positive blood vessels in each group. Transplanted hASCs were detected only in the transplantation group. Merged immunofluorescence images demonstrated that hASCs localized circumferentially in the CD31-positive blood vessels (Fig. 6b). Lumen formation in the wound was often observed in the transplantation group (Fig. 6b). The average CD31-positive area was significantly higher in the transplantation group ( $6.60 \pm 1.96\%$ ) compared with that of the control group ( $3.15 \pm 0.84\%$ ) ( $n = 4$ ) (Fig. 6d).

## 4. Discussion

Direct injection of hASCs into wounds promotes healing [23,24], although the hASCs are relatively unstable [9,10]. Considering the potential problems of immunorejection, autologous hASCs are considered the best source. However, isolation of autologous hASCs from diabetic patients is not a good choice because preparation of hASC sheets requires several weeks and exposes patients to risk of adverse effects such as severe diabetic complications, laparotomy dehiscence caused by impaired wound healing, and infection. Therefore, we consider using allogenic rather than autologous hASCs in future clinical trials. Moreover, in allogenic

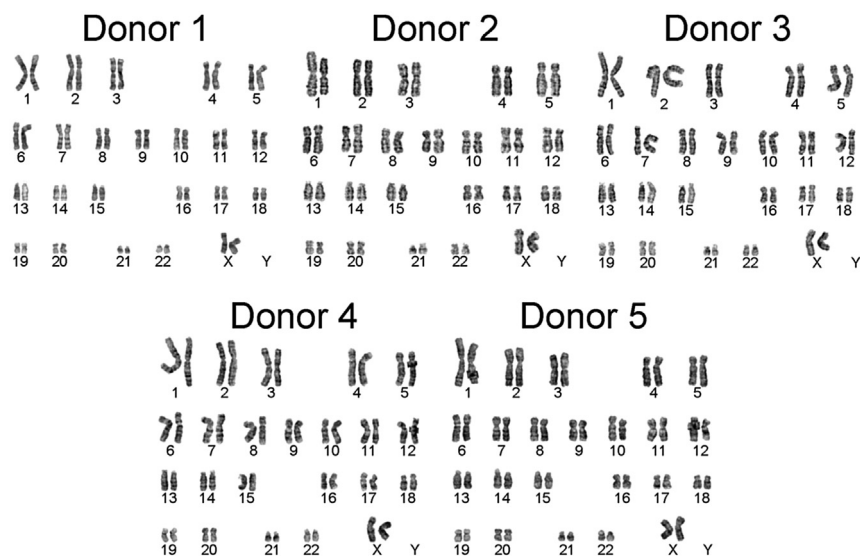
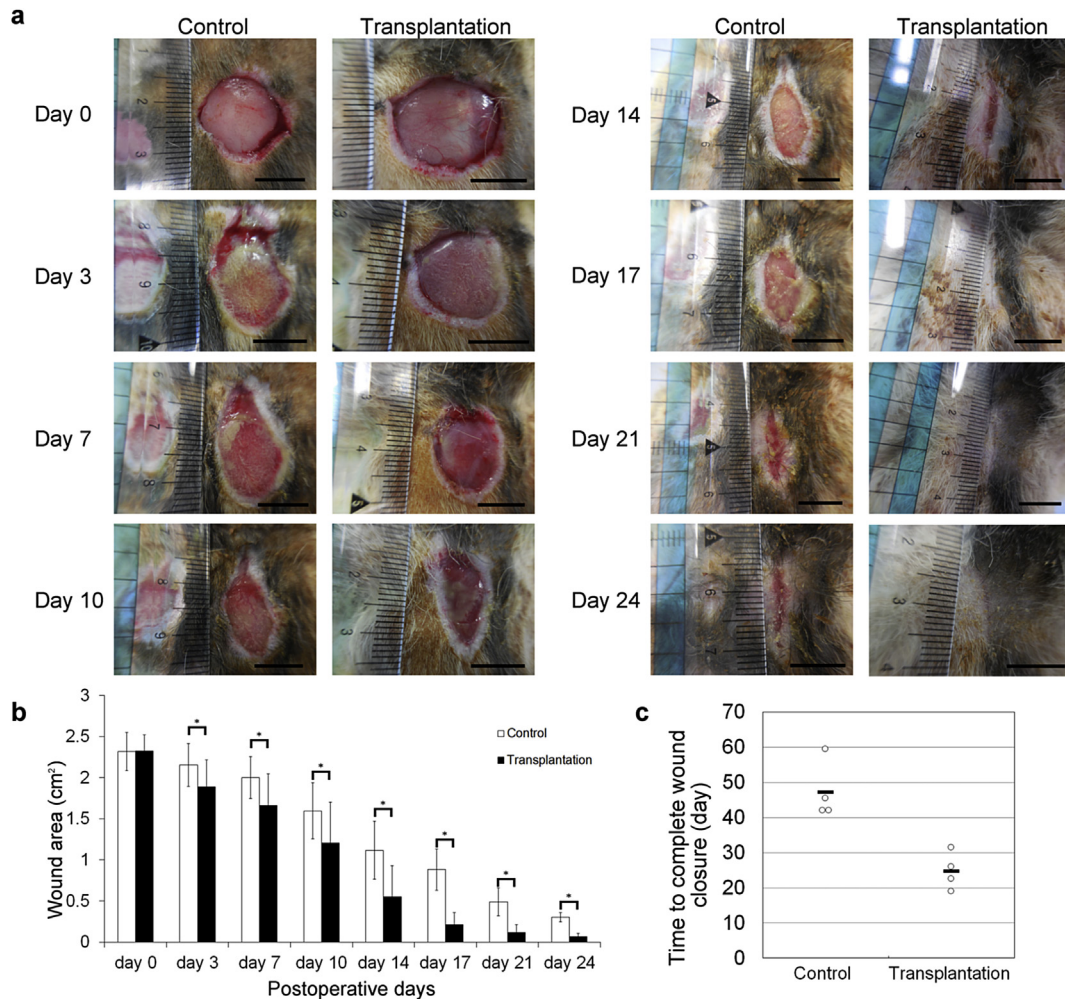


Fig. 4. G-banding of hASCs (Donors 1–5) at Passage 4 after long-term (31–136 days) cryopreservation revealed that the number, banding, and shape of the chromosomes were normal.



**Fig. 5.** Wound closure with or without a transplanted hASC sheet. (a) Representative macroscopic images of the wounds in the transplantation and control groups ( $n = 4$  each). Scale bars = 1 cm. (b) The average wound area of the transplantation group was significantly smaller compared with that of the control group, starting 3 days after transplantation.  $*p < 0.05$ . (c) The average complete wound-closure time of the transplantation group was significantly shorter compared with that of the control group.  $*p < 0.05$ . The values shown represent the mean  $\pm$  SD.

transplantation, we can select the most effective lot from among several lots to improve treatment. Thus, MSC markers that serve to assess the treatment effects are needed. However, such markers are not available. Therefore, we aimed to identify such markers to improve treatment.

We collected human subcutaneous adipose from patients who were undergoing mastectomy because liposuction procedures are rarely performed in our hospital. Although these samples were collected from patients with cancer, chromosomal tests and G-banding did not detect genetic abnormalities. Moreover, there are no phenotypic differences between hASCs isolated from patients with cancer and those from healthy subjects such as self-renewal, surface-marker expression, and ability to differentiate into different cell lineages [25]. Previous studies of wound healing using hASC sheets employed animal models with full-thickness skin defects 10–12 mm in diameter that tend to heal well [21,26]. In contrast, here we created large full-thickness skin defects (15-mm in diameter) on the backs of ZDF rats. Given the size of the skin defects and the animal models, this study focused on the effects of hASC sheets on larger wounds compared with those used in previous studies [21,26]. Surprisingly, in the present study, xenogeneic transplantation of hASC sheets enhanced wound healing in ZDF rats. Moreover, the clinical signs of immunorejection such as

erythema, inflammation, and necrosis [27,28] were not detected here. Further studies are therefore required to determine whether the hASC sheets suppress immunorejection.

Wound healing is a multifactorial process that involves inflammation, reepithelialization, angiogenesis, extracellular matrix deposition, and tissue remodeling [5], which requires growth factors. ASCs were found to secrete angiogenic growth factors in vitro and in vivo and not only contribute to cutaneous regeneration but also participate in new vessel formation [23]. Here, we show that VEGF, KGF, FGF, IGF-1, HGF, PDGF-BB, and EGF were secreted by hASCs into the conditioned medium. These growth factors play important roles in angiogenesis and wound healing [29,30]. The activities of growth factors are significantly impaired in patients with diabetes [5]; thus, we hypothesized that the secretion of growth factors is important for estimating the efficacy of hASCs for further transplantation therapy. It is known that VEGF is the most effective and specific growth factor that regulates angiogenesis [31,32]. Our previous study suggests that VEGF signaling stimulated angiogenesis and wound healing [16,33]. Previous studies reported that the high expression levels of angiogenic growth factors increased the rate and degree of granulation tissue and capillary formation and thus accelerated wound healing [23,34,35]. In the present study, we selected Donor 4 for

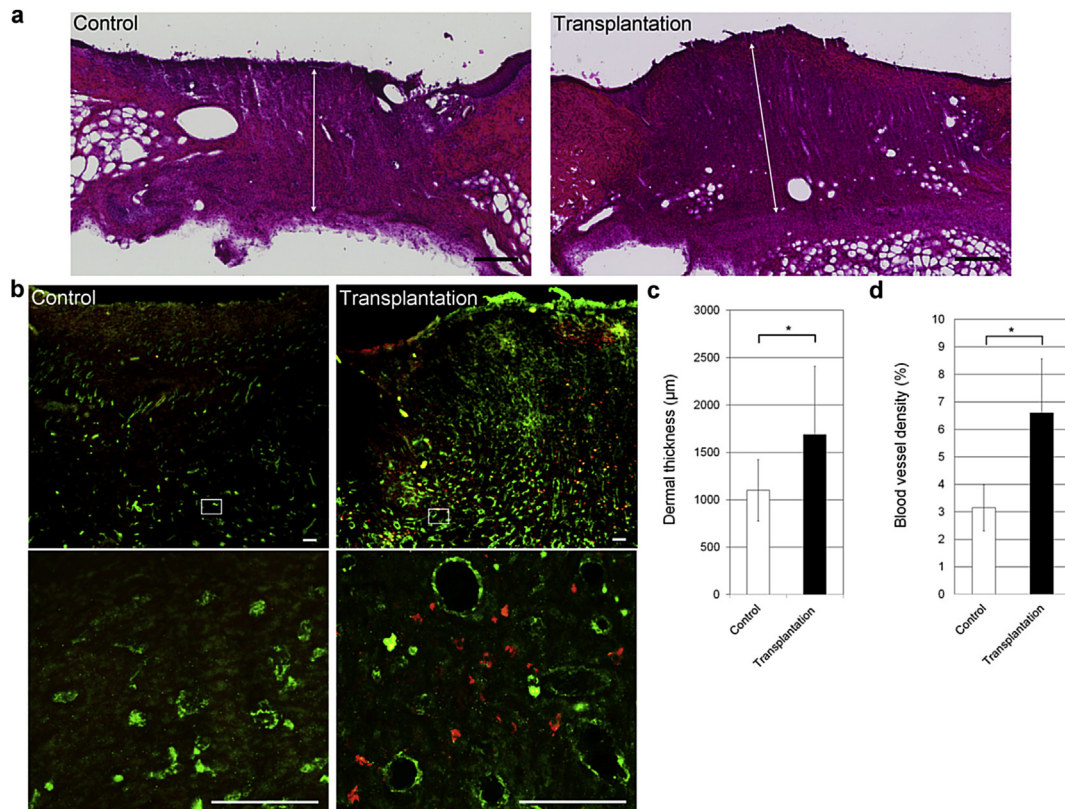


**Fig. 6.** Histological analysis of wounds treated with or without hASC sheets. (a) Representative histological images of H–E-stained wounds on day 14 after transplantation. Scale bars = 500 μm. (b) The upper section is low-power field photos. Scale bars = 100 μm. The below section is high-power field photos. Scale bars = 50 μm. In the control group, only CD31-positive areas (green) were observed. In the transplantation group, areas positive for STEM 121 (red) were detected along the periphery of the CD31-positive endothelial cells (green). (c) Dermal thickness in the transplantation group was significantly higher compared with that of the control group (n = 4) on day 14. \**p* < 0.05. The values represent the mean ± SD. (d) The upper section is low-power field photos. Scale bars = 100 μm. The below section is high-power field photos. Scale bars = 50 μm. The densities of blood vessels in the wound area were measured on day 14 after transplantation and were calculated by dividing the area of CD31-positive vessels by the total area. Scale bars = 50 μm \**p* < 0.05. The values shown represent the mean ± SD.

transplantation because the cells secreted growth factors and the levels of VEGF were the highest among the samples.

The present study shows that the time required for complete wound healing was significantly shorter, blood vessel density was significantly higher, and dermal thickness was significantly increased in the transplantation group compared with those of the control group. Thinner skin and reduced density of capillaries in the dermal layer of patients with diabetes are common causes of impaired wound healing that lead to lower-limb amputation [36]. Here, blood vessel density in the wound area was significantly higher and mature vessels with lumen formation were more frequent in the transplantation group than in the control group. These findings suggest that neovascularization was accelerated in the transplantation group and the mechanism involved signaling by growth factors secreted by the hASCs.

To summarize, the results of the present study suggest that the hASCs accelerated wound healing by thickening the dermis and neovascularizing the wound area. These findings led us to conclude that we have established the optimum protocol for generating hASC sheets that significantly accelerate wound healing. Our experimental system using ZDF rats may serve as a valuable model for evaluating the efficacy of human cell tissue-based products (hCTPs). Moreover, this model may contribute to the verification of the clinical efficacy of hCTPs and the identification of factors produced by hCTPs that mediate their beneficial effects.

## 5. Conclusions

We established an optimum protocol for generating hASC sheets and a system to evaluate their effects using a rat xenograft model of obese diabetes. Xenogeneic hASC sheet transplantation combined with artificial skin accelerated the healing of large wounds through promoting angiogenesis and the paracrine effects by secreted growth factors.

## Conflicts of interest

Teruo Okano is a founder and Director of the Board, CellSeed, Inc. and holds technology licenses and patents from Tokyo Women's Medical University. Teruo Okano is a shareholder of CellSeed, Inc. Tokyo Women's Medical University who receives research funds from CellSeed, Inc. The other authors disclose no financial relationships relevant to this publication.

## Acknowledgments

We are very grateful to Prof. Takashi Yamaki, Dr. Masahiro Shibata, and Dr. Miho Kirita of Plastic Surgery of Tokyo Women's Medical University for collecting adipose tissue. We also thank Prof. Takako Kamio, Dr. Eiichiro Noguchi, Dr. Tetsuya Daichi, and Dr. Hiroko Tsukada of Surgery of Tokyo Women's Medical University for collecting blood from donors. We are grateful to Ms. Hozue



Kuroda of the Institute of Advanced Biomedical Engineering and Science at Tokyo Women's Medical University for excellent technical support. We would like to express our gratitude to Prof. Taichi Ezaki of the Department of Anatomy and Developmental Biology of Tokyo Women's Medical University School of Medicine for expert technical advice and support in immunohistochemistry. We also thank Dr. Kazuki Ikura of the Diabetic Center of Tokyo Women's Medical University School of Medicine for expert advice on diabetic feet. This study was supported by the Creation of Innovation Centers for Advanced Interdisciplinary Research Areas Program of the Project for Developing Innovation Systems "Cell Sheet Tissue Engineering Center (CSTEC)" from the Ministry of Education, Culture, Sports, Science and Technology (MEXT), Japan. This work was partially supported by JSPS KAKENHI Grant Number 15K11224.

## References

- [1] International Diabetes Federation. IDF diabetes atlas. 7 ed. Brussels, Belgium: International Diabetes Federation; 2015.
- [2] Boulton AJ, Vileikyte L, Ragnarson-Tennvall G, Apelqvist J. The global burden of diabetic foot disease. *Lancet* 2005;366:1719–24.
- [3] Frykberg RG, Zgonis T, Armstrong DG, Driver VR, Giurini JM, Kravitz SR, et al. Diabetic foot disorders. A clinical practice guideline (2006 revision). *J Foot Ankle Surg* 2006;45:S1–66.
- [4] Martin P. Wound healing—aiming for perfect skin regeneration. *Science* 1997;276:75–81.
- [5] Falanga V. Wound healing and its impairment in the diabetic foot. *Lancet* 2005;42:239–47.
- [6] Matsuda K, Suzuki S, Isshiki N, Ikada Y. Re-freeze dried bilayer artificial skin. *Biomaterials* 1993;14:1030–5.
- [7] Zuk P. The ASC: critical participants in paracrine-mediated tissue health and function. In: Andrades JA, editor. *Regenerative medicine and tissue engineering*. Rijeka: InTech Open; 2013. <http://dx.doi.org/10.5772/55545>.
- [8] Wu Y, Chen L, Scott PG, Tredget EE. Mesenchymal stem cells enhance wound healing through differentiation and angiogenesis. *Stem Cells* 2007;10:2648–59.
- [9] Yang J, Yamato M, Kohno C, Nishimoto A, Sekine H, Fukai F, et al. Cell sheet engineering: recreating tissues without biodegradable scaffolds. *Biomaterials* 2005;26:6415–22.
- [10] Zhang M, Methot D, Poppa V, Fujio Y, Walsh K, Murry CE. Cardiomyocyte grafting for cardiac repair: graft cell death and anti-death strategies. *J Mol Cell Cardiol* 2001;33:907–21.
- [11] Okano T, Yamada N, Sakai H, Sakurai Y. A novel recovery system for cultured cells using plasma-treated polystyrene dishes grafted with poly(N-isopropylacrylamide). *J Biomed Mater Res* 1993;27:1243–51.
- [12] Ohki T, Yamato M, Murakami D, Takagi R, Yang J, Namiki H, et al. Treatment of oesophageal ulcerations using endoscopic transplantation of tissue-engineered autologous oral mucosal epithelial cell sheets in a canine model. *Gut* 2006;55:1704–10.
- [13] Iwata T, Yamato M, Tsuchioka H, Takagi R, Mukobata S, Washio K, et al. Periodontal regeneration with multi-layered periodontal ligament-derived cell sheets in a canine model. *Biomaterials* 2009;30:2716–23.
- [14] Nishida K, Yamato M, Hayashida Y, Watanabe K, Yamamoto K, Adachi E, et al. Corneal reconstruction with tissue-engineered cell sheets composed of autologous oral mucosal epithelium. *N Engl J Med* 2004;12:1187–96.
- [15] Miyahara Y, Nagaya N, Kataoka M, Yanagawa B, Tanaka K, Hao H, et al. Monolayered mesenchymal stem cells repair scarred myocardium after myocardial infarction. *Nat Med* 2006;12:459–65.
- [16] Kato Y, Iwata T, Morikawa S, Yamato M, Okano T, Uchigata Y. Allogenic transplantation of an adipose-derived stem cell sheet combined with artificial skin accelerates wound healing in a rat wound model of type 2 diabetes and obesity. *Diabetes* 2015;64:2723–34.
- [17] Dorsett-Martin WA. Rat models of skin wound healing: a review. *Wound Repair Regen* 2004;12:591–9.
- [18] Schreml S, Babilas P, Fruth S, Orso E, Schmitz G, Mueller MB, et al. Harvesting human adipose tissue-derived adult stem cells: resection versus liposuction. *Cytotherapy* 2009;11:947–57.
- [19] Yoshimura H, Muneta T, Nimura A, Yokoyama A, Koga H, Sekiya I. Comparison of rat mesenchymal stem cells derived from bone marrow, synovium, periosteum, adipose tissue, and muscle. *Cell Tissue Res* 2007;327:449–62.
- [20] Washio K. Improved enzymatic treatment for accurate cell counting from extracellular matrix-rich periodontal ligament cell sheets. *Int J Oral Maxillofac Implants* 2014;29:e117–21.
- [21] Cerqueira MT, Pirraco RP, Santos TC, Rodrigues DB, Frias AM, Martins AR, et al. Human adipose stem cells cell sheet constructs impact epidermal morphogenesis in full-thickness excisional wounds. *Biomacromolecules* 2013;14:3997–4008.
- [22] Dominici M, Le Blanc K, Mueller I, Slaper-Cortenbach I, Marini FC, Krause DS. Minimal criteria for defining multipotent mesenchymal stromal cells. The International Society for Cellular Therapy position statement. *Cytotherapy* 2006;8:1–7.
- [23] Nie C, Yang D, Xu J, Si Z, Jin X, Zhang J. Locally administered adipose-derived stem cells accelerate wound healing through differentiation and vasculogenesis. *Cell Transpl* 2011;20:205–16.
- [24] Shin L, Peterson DA. Human mesenchymal stem cell grafts enhance normal and impaired wound healing by recruiting existing endogenous tissue stem/progenitor cells. *Stem Cells Transl Med* 2013;2:33–42.
- [25] Garcia-Contreras M, Vera-Donoso CD, Hernandez-Andreu JM, Garcia-Verdugo JM, Oltra E. Therapeutic potential of human adipose-derived stem cells (ADSCs) from cancer patients: a pilot study. *PLoS One* 2014;9:e113288.
- [26] Lin YC, Grahovac T, Oh SJ, Ieraci M, Rubin JP, Marra KG. Evaluation of a multi-layer adipose-derived stem cell sheet in a full-thickness wound healing model. *Acta Biomater* 2013;9:5243–50.
- [27] Falanga V, Margolis D, Alvarez O. Human Skin Equivalent Investigators group. Rapid healing of venous ulcers and lack of clinical rejection with an allogenic cultured human skin equivalent. *Arch Dermatol* 1998;134:293–300.
- [28] Briscoe DM, Dharnidharka VR, Isaacs C. The allogenic response to cultured human skin equivalent in the hu-PBL-SCID mouse model of skin rejection. *Transplantation* 1999;67:1590–9.
- [29] Barrientos S, Stojadinovic O, Golinko MS, Brem H, Tomic-Canic M. Growth factors and cytokines in wound healing. *Wound Repair Regen* 2008;16:585–601.
- [30] Rehman J, Traktuev D, Li J, Merfeld-Claus S, Temm-Grove CJ, Bovenkerk JE, et al. Secretion of angiogenic and antiapoptotic factors by human adipose stromal cells. *Circulation* 2004;109:1292–8.
- [31] Nakagami H, Maeda K, Morishita R, Iguchi S, Nishikawa T, Takami Y, et al. Novel autologous cell therapy in ischemic limb disease through growth factor secretion by cultured adipose tissue-derived stromal cells. *Arterioscler Thromb Vasc* 2005;25:2542–7.
- [32] Nie C, Morris SF. Local delivery of adipose-derived stem cells via acellular dermal matrix as a scaffold: a new promising strategy to accelerate wound healing. *Med Hypotheses* 2009;72:679–82.
- [33] Kaibuchi N, Iwata T, Yamato M, Okano T, Ando T. Multipotent mesenchymal stromal cell sheet therapy for bisphosphonate-related osteonecrosis of the jaw in a rat model. *Acta Biomater* 2015;16:30299.
- [34] Nie C, Zhang G, Yang D, Liu D, Xu J, Zhang J. Targeted delivery of adipose-derived stem cells via acellular dermal matrix enhances wound repair in diabetic rats. *J Tissue Eng Regen Med* 2015;9:224–35.
- [35] Park IS, Chung PS, Ahn JC. Adipose-derived stromal cell cluster with light therapy enhance angiogenesis and skin wound healing in mice. *Biochem Biophys Res Commun* 2015;462:171–7.
- [36] Petrofsky JS, McLellan K, Bains GS, Prowse M, Ethiraju G, Lee S, et al. Skin heat dissipation: the influence of diabetes, skin thickness, and subcutaneous fat thickness. *Diabetes Technol Ther* 2008;10:487–93.